

reactions for both the  $^4E$  and  $^4B_2$  intermediates (the latter required by the wavelength dependence) would, in principle, justify any amount of the *cis-fac* and *cis-mer* isomers, and even the possible presence of *trans-mer* product.

The associative model assumes formation of a seven-coordinate intermediate, by solvent approach *trans* to the labilized ligand,<sup>2-4</sup> and the expectations are substantially those of a concerted, edge-displacement mechanism. On a statistical basis, axial labilization ( $^4E$ ) should produce a 1:1 ratio of *cis-mer* ( $H_2O$  entry on the  $NH_3-NH_3$  edges) and *cis-fac* isomers (attack on the  $NH_3-CN$  edges). For release of equatorial  $NH_3$  ( $^4B_2$ ), statistical *trans* coordination would result in a 1:2:1 distribution of *cis-mer*, *cis-fac*, and *trans-mer* species, respectively.

This mechanism also accounts for the stereochemical findings in terms of predominant  $^4E$  photoreactivity. The percentage of *cis-fac* product, higher than statistical, may be attributed to preferential migration of the negatively charged cyanide ligands away from the incoming solvent molecule. The lack of *trans-mer* product (related to  $^4B_2$ ) may be also explained by electrostatic repulsion, hindering access of water between the  $CN^-$  groups. A possible incongruence of this description is that at higher excitation energies (assumed to enhance the involvement of  $^4B_2$ , as suggested by the wavelength dependence) the proportion of *cis-fac* isomer should increase, in contrast with observation.

To sum up, the stereochemistry of the photoproducts and, roughly, their distribution are consistent with both mechanisms, if chemical deactivation is thought to take place mainly in the lowest excited quartet. Neither model satisfactorily accounts for the wavelength dependence and for the missing *trans-mer* product. A more detailed analysis is virtually impossible since (i) there are too many unknown parameters and (ii) the

adopted  $D_{4h}$  symmetry may well be an oversimplification.

A survey of the available data on the photostereochemistry of  $NH_3$  aquation in other chromium(III) tetraammines shows that a definitive choice between the two models cannot be made yet. The behavior of *cis*- $Cr(NH_3)_4F_2^+$  is more compatible with the Vanquickenborne-Ceulemans theory;<sup>4</sup> that of *trans*- $Cr(NH_3)_4F_2^+$  is consistent with both mechanisms,<sup>4</sup> while for *trans*- $Cr(NH_3)_4(CN)_2^+$  the results are best rationalized by the edge-displacement approach.<sup>3,37</sup> Several aspects of the stereochemistry are therefore still elusive, specially in systems of the present complexity. Regardless of the mechanistic details, independent studies of solvent<sup>38</sup> and high-pressure<sup>39</sup> effects indicate that, at least for cationic chromium(III) complexes, associative, or concerted, photoreaction paths are preferred.

**Acknowledgment.** The authors wish to thank Dr. A. Ceulemans for helpful discussion. The National Research Council of Italy (CNR) is gratefully acknowledged for financial support.

**Registry No.** *cis*- $Cr(NH_3)_4(CN)_2^+$ , 77981-98-7;  $Cr(NH_3)_3(H_2O)(CN)_2^+$  (1,2-CN-3- $H_2O$  isomer), 86023-23-6;  $Cr(NH_3)_3(H_2O)(CN)_2^+$  (1,2-CN-6- $H_2O$  isomer), 76333-25-0;  $Cr(NH_3)_3(H_2O)_3^{3+}$ , 85404-37-1.

- (37) Application of the dissociative model to the higher excited quartet of *trans*- $Cr(NH_3)_4(CN)_2^+$ ,  $^4E_g$ , incorrectly considered reaction through both an excited-state and a ground-state bipyramid, leading to *cis-mer* and *trans-mer* dicyanoaquo products, respectively. Such an intermediate is instead expected to react in its ground state ( $^4B_2$ ) and to yield *cis-mer* product only.<sup>34</sup> This difference, however, does not modify the conclusions drawn in ref 3.
- (38) Cusumano, M.; Langford, C. H. *Inorg. Chem.* **1978**, *17*, 2222.
- (39) Angermann, K.; van Eldik, R.; Kelm, H.; Wasgestian, F. *Inorg. Chem.* **1981**, *20*, 955.

Contribution from the Department of Chemistry and Department of Mathematics, St. Patrick's College, Maynooth, Co. Kildare, Ireland

## Mollweide Projections: Molecular Orbital Symmetries on the Spherical Shell, Tetrahedral and Other Symmetries, and $\delta$ Orbitals in Metal Clusters

C. M. QUINN,\* J. G. MCKIERNAN, and D. B. REDMOND

Received October 4, 1982

The pictorial approach to the generation of group orbitals based on the representation of basic symmetry requirements with Mollweide projections is further developed. General rules are given for the application of this technique to the major classes of structures commonly found for molecules. The utility of the technique for the analysis and discussion of  $\sigma$ -,  $\pi$ -, and  $\delta$ -type interactions of atomic orbitals is illustrated.

Recently<sup>1</sup> we have proposed the use of a cartographic device, the Mollweide projection, for the construction and presentation of symmetry-adapted functions for molecular point-group structures within the generator orbital approach to the LCAO approximation. In this paper we demonstrate the utility of the method for the other commonly occurring molecular symmetries than  $\hat{O}_h$  and illustrate the simple manner in which  $\sigma$ -,  $\pi$ -, and  $\delta$ -type interactions can be analyzed and discussed within the same framework.

The essential philosophy of the generator orbital approach<sup>2,3</sup> is the reproduction, with the use of local functions (the atomic orbitals) sited at atomic positions about a chosen origin de-

termined by the molecular point group, of the nodal structures of actual or imagined orbitals sited at that chosen origin. The role of these generator orbitals is the detailing of the possible basis function symmetries as nodal patterns for the point group irreducible representations. This is so because the set of atomic orbitals of any atom sited at the origin (basis functions, in the orbital spherical harmonic components, of the irreducible representations of the spherical group  $\hat{R}_3$ ) provide an overcomplete set of functions from which can be chosen compo-

\* To whom correspondence should be addressed at the Department of Chemistry.

- (1) C. M. Quinn, J. G. McKiernan, and D. B. Redmond, *J. Chem. Educ.*, in press.
- (2) D. K. Hoffman, K. Ruedenberg, and J. G. Verkade, *J. Chem. Educ.* **54**, 590 (1977).
- (3) D. K. Hoffman, K. Ruedenberg, and J. G. Verkade, *Struct. Bonding (Berlin)* **33**, 57 (1977).

**Table I.** Cubic Harmonics for the Representation of All the Irreducible Representations of  $O_h$  and the Origins of These Unique Symmetries in the Subspaces of  $R_3^a$

$A_{1g}$	S	(000)
$T_{1u}$	P	(001), (100), (010)
$E_g$	D	2(002) - (200) - (020), (200) - (020)
$T_{2g}$	D	(110), (011), (101)
$A_{2u}$	F	(111)
$T_{2u}$	F	(201) - (021), (120) - (102), (012) - (210)
$T_{1g}$	G	(130) - (310), (013) - (031), (301) - (103)
$E_u$	H	2(113) - (311) - (131), (311) - (131)
$A_{2g}$	I	(240) + (024) + (402) - (420) - (042) - (204)
$A_{1u}$	L	(351) + (135) + (513) - (531) - (153) - (315)

<sup>a</sup> The notation  $(ijk)$  is due to Elert<sup>11</sup> and translates as  $x^i y^j z^k$ .

**Table II.** Mappings, as Direct Sums, of the Irreducible Subspaces of the Spherical Group  $R_3$  on the Irreducible Subspaces of  $O_h^a$

S	$A_{1g}$	H	$E_u + 2T_{1u} + T_{2u}$
P	$T_{1u}$	I	$A_{1g} + A_{2g} + E_g + T_{1g} + 2T_{2g}$
D	$T_{2g} + E_g$	J	$A_{2u} + E_u + 2T_{1u} + 2T_{2u}$
F	$A_{2u} + T_{1u} + T_{2u}$	K	$A_{1g} + 2E_g + 2T_{1g} + 2T_{2g}$
G	$A_{1g} + E_g + T_{1g} + T_{2g}$	L	$A_{1u} + A_{2u} + E_u + 3T_{1u} + 2T_{2u}$

<sup>a</sup> In  $R_3$  the subspaces are listed with use of the symbolism appropriate to atomic orbitals: Mulliken symbols are used to distinguish the irreducible representations of  $O_h$ . The list is terminated when all the irreducible representations of  $O_h$  have been involved in the direct sums.

nents appropriate to the irreducible representations of point groups of less than spherical symmetry. In our Mollweide projection technique these basic central patterns are presented as two-dimensional maps and the required LCAO functions are obtained for particular point-group molecular symmetries from these universal charts.

The common molecular symmetries divide into two types. There are the molecular symmetries based on cubic geometry, the two most important examples being  $O_h$  and  $T_d$ , and the second type encompassing the dihedral groups and subgroups such as  $C_{nv}$ .<sup>4a</sup> For the cubic point groups the cubic harmonics<sup>4b</sup> are the appropriate linear combinations of the general spherical harmonics to present as Mollweide projections, since they exhibit the required transformation properties of the basis set for the degenerate irreducible subspaces of  $O_h$  and  $T_d$ . For the other class of molecular symmetries the general functions should be used.

### Basis Functions for the Cubic Groups $O_h$ and $T_d$

For the groups  $O_h$  and  $T_d$  of the  $MX_6$  and  $MX_4$  structures all the  $\sigma$ - and  $\pi$ -type molecular orbital symmetries that can be constructed from the s and p atomic orbitals at each ligand position can be obtained from the Mollweide projections of the s, p, and d spherical harmonics and the f and g specifically cubic harmonics. The representation of all the irreducible symmetries of  $O_h$  in this manner, however, requires the use of various spherical harmonics up to the L level. The functional forms for these functions are presented in Table I with use of Elert's notation<sup>5</sup> together with their conventional Mulliken labels and the origins of these unique symmetries in  $R_3$ . Note that the subspaces of  $R_3$  map homomorphically onto the lower order subgroups of  $O_h$  as given in Table II. And so repetitions of symmetries occur with increasing order of the spherical harmonics. Thus, our attention is confined

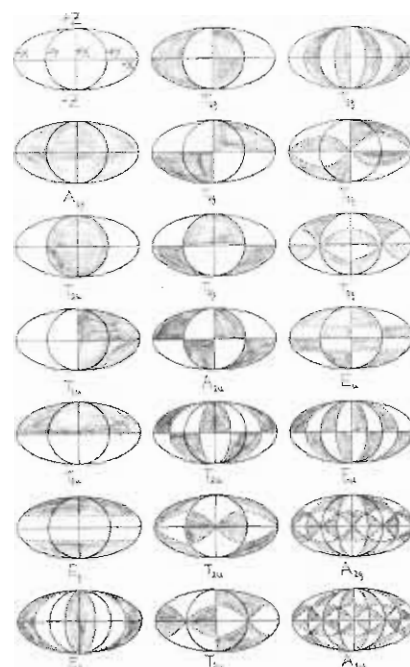


**Figure 1.** Basic geometry of the Mollweide projection and basis functions for the irreducible representations of  $O_h$  in this form with the cubic harmonics.

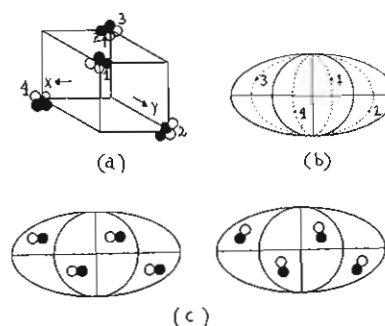


**Figure 2.** (a) Conventional, cube-based, representation of tetrahedral geometry and the  $p\pi$  ligand orbital set. (b) Tetrahedral geometry as a Mollweide projection. (c)  $p\pi$  ligand set in projection form (the  $p\pi$  orbitals divide as  $\pi_l^\phi$  along lines of longitude and  $\pi_l$  along lines of latitude).

to the unique representations of Table I, and these are presented as Mollweide projections in Figure 1 with areas of positive function amplitude identified by shading.

For  $O_h$  symmetry  $MX_6$  structures the generation of  $\sigma$ - and  $\pi$ -type group orbitals has been considered in detail elsewhere.<sup>1</sup> In Figure 2 the atomic positions for  $T_d$ -symmetry molecules and a set of general  $p\pi$  ligand orbitals are presented in the conventional manner (Figure 2a) at the appropriate corners of a cube and also as Mollweide projections for the presentation of the basic geometry (Figure 2b) and the  $p\pi$  orbital locations and orientations (Figure 2c). The construction of  $\sigma$ -type group orbitals from local s or  $p\sigma$  oriented ligand atomic orbitals follows directly from the superimposition of, for example, Figure 2b (assume that the black dots defining the atomic positions also identify s orbitals or  $p\sigma$  lobes of given sign) on the set of Mollweide projections of Figure 1. For the  $p\pi$  set of ligand orbitals in Figure 2c this simple superimposition procedure is not sufficient to give directly the coefficients of the group orbital components because for cubic symmetries lower than  $O_h$  the locally mutually orthogonal ligand  $p\pi$  orbitals are not simply disposed in general to be tangential or perpendicular to nodal or constant contour lines of the Mollweide projections.

(4) (a) This division and the use of the appropriate spherical or cubic harmonic set is preferable, since it yields a consistent coordinate system, even through many of the second type of group are subgroups of  $O_h$  if the essential requirements in  $O_h$  of interchangeability of x, y, and z is maintained by suitable orientation of the group geometry in the cube, e.g. the siting of  $C_{3v}$  geometry about the (111) axis. (b) H. Bethe, *Ann. Phys. (Leipzig)*, 3, 133 (1929).

(5) W. Elert, *Z. Phys.*, 51, 8 (1928).

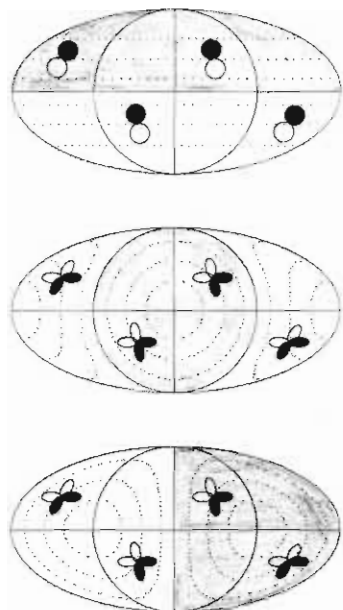


**Figure 3.** Results of the superimposition of Figure 2c on the p subset of the basic set of projections of Figure 1. Only in the first diagram is there a simple result involving single local functions ( $\pi_i^\theta$ ) at each atomic position.

This difficulty is manifest in Figure 3. The Mollweide projections for the  $T_2$  set of  $\hat{T}_d$  symmetry are presented with contour lines defining equal amplitudes of the central p functions on the unit sphere. For the first projection the  $p\pi$  orbitals in the horizontal direction can be excluded since they exhibit a net zero overlap with the projection, and the simple superimposition process leads to the correct group orbital combination transforming as a central  $p_z$  function. For the remaining group orbitals this does not work: none of the local  $p\pi$  orbitals are excluded by the superimposition of Figure 2c on the p set of Mollweide projections, and the coefficients of the individual components are left undetermined. The remedy required is implicit in the first diagram of Figure 3 for which the superimposition procedure does work. In that case the local functions do either lie tangentially along a contour line of the central function amplitude or lie normal to such a line, and so the tangentially oriented components can be excluded. For the remaining group orbitals of the  $T_2$  set, and generally for  $p\pi$  interactions, the correct components on the ligands are the resultants obtained by taking the linear combinations of the local  $p\pi$  sets which yield the same functional forms lying along the normals to contours passing through the ligand positions.

The property of the central function that is being matched in this process is the gradient, locally on each Mollweide projection the lines of the greatest slope at the ligand positions. The most convenient mathematical method for determining these directions at each ligand position and thereby the appropriate coefficients for the group orbital components ( $\pi_i^\theta$  along lines of longitude with positive lobe pointing south, and  $\pi_i^\phi$  along lines of latitude with positive lobe pointing east through each ligand position "i") has been given recently by Stone.<sup>6,7a</sup> in the course of the development of a novel cluster theory. The taking of the gradient of the central functions is equivalent to the defining of the surface harmonics on the unit sphere; in each case the surface function obtained as the partial derivative with respect to  $\theta$  yields at each ligand position

(6) A. J. Stone, *Mol. Phys.*, **41**, 1339 (1980).

(7) (a) A. J. Stone, *Inorg. Chem.*, **20**, 563 (1981). (b) This procedure is formally the same as that used in the angular-overlap method of C. K. Jørgensen and C. E. Schäffer (for example, *Mol. Phys.*, **9**, 401 (1965) and later publications) and accounts for the appearance of the tensor harmonic functions in that theory as explained in ref 8b.

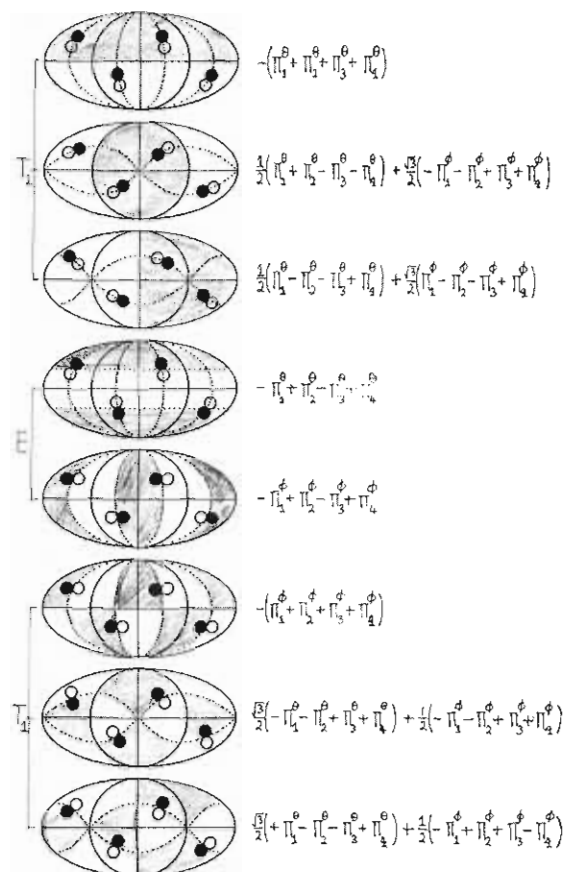


**Figure 4.** Basic functions for the  $\pi$  group orbitals in tetrahedral symmetry transforming as the  $T_2$ , E, and  $T_1$  irreducible representations as Mollweide projections with resultant components at each site in the direction of greatest slope and as linear combinations of  $\pi_i^\theta$  and  $\pi_i^\phi$  along great-circle axes of antisymmetry of the central function.

the appropriate coefficients for the  $\pi_i^\theta$  components, while the surface function obtained as the partial derivative of the central function with respect to the azimuthal angle yields the coefficients for the  $\pi_i^\phi$  components.<sup>7b</sup>

Pictorially for the two classes of point group with which we are concerned in this paper, these gradient directions and the orientations of the appropriate resultant  $p\pi$  functions at each ligand position can be determined directly from the Mollweide projections. In all cases ligand positions can be chosen to lie on great circles of the unit sphere which are either axes of symmetry or axes of antisymmetry of the central functions generating the appropriate group orbital symmetries. The local  $p\pi$  resultant components at such ligand positions are required to lie along the directions of axes of symmetry and at  $90^\circ$  to axes of antisymmetry oriented so that positive and negative phases of the local functions exhibit maximum overlaps with the central function phases.<sup>8</sup> Moreover it follows and it is implicit in Stone's analysis also that the local rotation through  $90^\circ$  in the same sense at each ligand position of the components of a group orbital also yields a group orbital.

In Figure 4 the Mollweide projections corresponding to the  $\pi$ -type group orbitals of the  $\hat{T}_d$ -symmetry structure that are consistent with these statements are presented. The coefficients of the  $\pi_i^\theta$  and  $\pi_i^\phi$  individual components are also listed against each group orbital projection, and these have been obtained from the corresponding surface harmonics given by Stone.<sup>7a</sup> In each diagram two great circles are involved and each passes through two ligand positions and two axial points  $\pm\hat{e}_x$  or  $\pm\hat{e}_y$ ,

(8) (a) C. M. Quinn, J. G. McKiernan, and D. B. Redmond, *J. Chem. Educ.*, in press; (b) D. B. Redmond, C. M. Quinn, and J. G. McKiernan, *J. Chem. Soc., Faraday Trans. 2*, in press.

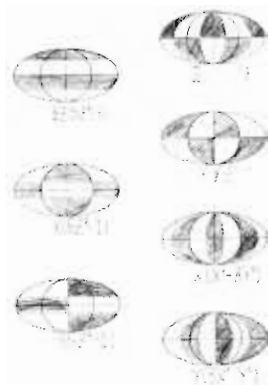


Figure 5. Mollweide projections of the general f spherical harmonics.

or  $\pm\hat{e}_z$ . These great circles are distinguished on the diagrams of Figure 4 by different broken-line patterns as described in the caption. The first three diagrams yield the  $T_2$ -type group orbitals transforming in the same manner as the central functions  $p_z$ ,  $p_x$ , and  $p_y$ . In these first three cases the great circles are axes of symmetry of the central functions. Local rotation of the resultant components through  $90^\circ$  in each case yields the  $T_1$  group orbitals, which transform as the  $f_{z(x^2-y^2)}$ ,  $f_{x(y^2-z^2)}$ , and  $f_{y(z^2-x^2)}$  central functions in which the same great circles encompassing the ligand positions are axes of antisymmetry of the central functions. The Mollweide projections and functional forms for these group orbitals are given in the last three diagrams of Figure 4. The remaining pair of group orbitals of E symmetry is obtained from the Mollweide projections of the central functions  $d_{z^2}$  and  $d_{x^2-y^2}$ , and this is an example of the unusual case in which the local rotations merely interchange the basis functions of the same degenerate irreducible symmetry. These group orbitals are presented in the middle two diagrams of Figure 4.

The  $MX_8 O_h$ -symmetry CsCl structure is not found for molecular material since other geometries are of lower total energies. The hypothetical cluster structure corresponds to two interlocked tetrahedral systems, and the irreducible symmetries for  $\pi$ -type ligand orbital interactions  $E_g$ ,  $E_u$ ,  $T_{1g}$ ,  $T_{1u}$ ,  $T_{2g}$ , and  $T_{2u}$  follow directly from the above analysis when the appropriate geometry is superimposed on the standard set of symmetry Mollweide projections of Figure 1.

#### Basis Functions for the Dihedral and Related Groups

The general set of spherical harmonics in the form of Mollweide projections provide a direct basis for the construction of symmetry-adapted functions as linear combinations of local ligand orbitals. The general set of s, p, and d spherical harmonics are unaltered for cubic systems, and these projections have been given already in Figure 1. The general f and g spherical harmonics are presented in Figures 5 and 6. For the dihedral groups up to  $D_{6h}$  and  $D_{6d}$  these sets of Mollweide projections are sufficient to permit the identification of all the group orbitals that can be formed from ligand s and p orbitals. Group orbitals of  $\sigma$  type are easily generated in all cases. There are two minor complications. For group orbitals formed as linear combinations of ligand orbitals sited at inequivalent positions on the unit sphere of the central function projections, it is necessary to modulate each term by the central function amplitudes at the ligand positions. Secondly, as the point-group symmetry diminishes, increasing homomorphisms are found in the mapping of the irreducible subspaces of the spherical group  $R_3$  onto the irreducible subspaces of the lower symmetry groups. This means that repetitions of symmetry can occur in the pictorial scheme for the generation of group orbitals from the Mollweide projections of the spherical harmonic basis functions of  $R_3$  before all the different kinds of symmetry have been identified. Such repetitions should be

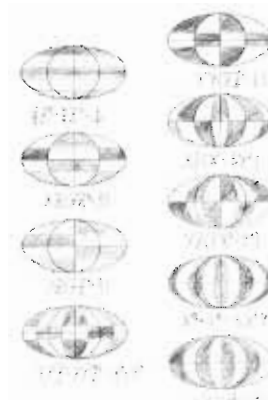


Figure 6. Mollweide projections of the general g spherical harmonics.

excluded while other cases are also possible and present no difficulties for the cases of  $\sigma$ -type interaction since the repeated ligand  $\sigma$  combinations are very easy to recognize.

Group orbitals of  $\pi$  type follow directly from  $\sigma$ -type functions. In the dihedral groups there are no symmetry operations that interchange  $z$ , the principal rotational axis of such groups, with either  $x$  or  $y$  and the simplest group orbitals of  $\pi$  type result when this distinction is maintained in the analysis. The gradient-dependent surface harmonic technique is valid of course, but because symmetry repetitions are difficult to exclude unless the simplest functions are identified, it is more convenient to exploit this unique property of  $z$  and also therefore the function space spanned by the  $\pi_i^\theta$  components on the unit sphere. Thus the group orbitals can be constructed solely from  $\pi_i^\theta$  or  $\pi_i^\phi$  components even though such combinations are of the same symmetries in many cases.<sup>8</sup> The  $\pi_i^\theta$  combinations result from the superimposition of the Mollweide projection for the  $\pi_i^\theta$  geometry on the projections that generate the distinct  $\sigma$ -type group orbitals, and the  $\pi_i^\phi$  combinations are then obtained from these new functions by locally rotating each  $\pi_i^\theta$  through  $\pi/2$ . The irreducible symmetries obtained in the first operation can be identified from the transformation properties of the product function of  $z$  with the central harmonics generating the  $\sigma$  group orbitals, while those resulting from the second operation are given by the direct products of these first irreducible symmetries with the group irreducible representation exhibiting traces +1 for proper rotations and traces -1 for improper rotations.

The analysis required for the cases of  $\sigma$  and  $\pi$  ligand interactions in  $C_{6v}$  symmetry illustrates these points. In  $C_{6v}$  six  $\sigma$ -type local functions (either s or  $p\sigma$  at each ligand position) generate six group orbitals. In Figure 7 these six symmetry-adapted functions are presented in projection form. One finds an s-like combination ( $A_1$  symmetry for the s,  $p_z$ ,  $d_{z^2}$ , and  $f_{z(5z^2-3)}$  projections),  $p_x$ - and  $p_y$ -like combinations ( $E_1$  symmetry for  $p_x/p_y$ ,  $d_{xy}/d_{yz}$ , and  $f_{y(5z^2-1)}/f_{x(5z^2-1)}$  projections),  $d_{xy}$ - and  $d_{x^2-y^2}$ -like combinations ( $E_2$  symmetry for the  $d_{xy}/d_{x^2-y^2}$  and  $f_{xyz}/f_{z(x^2-y^2)}$  projections), and finally an  $i_{xy(6x^4-20x^2y^2+6y^4)}$ -like combination ( $A_2$  symmetry).

For 12 local  $p\pi$  functions in  $C_{6v}$  symmetry the six group orbitals involving  $\pi_i^\theta$  components only on the ligands follow immediately from the  $\sigma$  analysis. These  $\pi^\theta$ -group orbitals are given in the first column of diagrams in Figure 8 while the  $\pi^\phi$ -group orbitals resulting from the first set by rotations through  $\pi/2$  are given in the second column. Note that this procedure generates the conventional sets of group orbitals that are obtained from standard group-theoretical techniques and that the modulation of  $\sigma$  functions carries through to the  $\pi$  (and later the  $\delta$ ) analysis. The results obtained by use of the surface harmonic procedure in such cases as  $C_{6v}$  symmetry are unnecessarily complicated because the canonical sets of  $\pi_i^\theta$  and  $\pi_i^\phi$  group orbitals of the same symmetries become mixed in

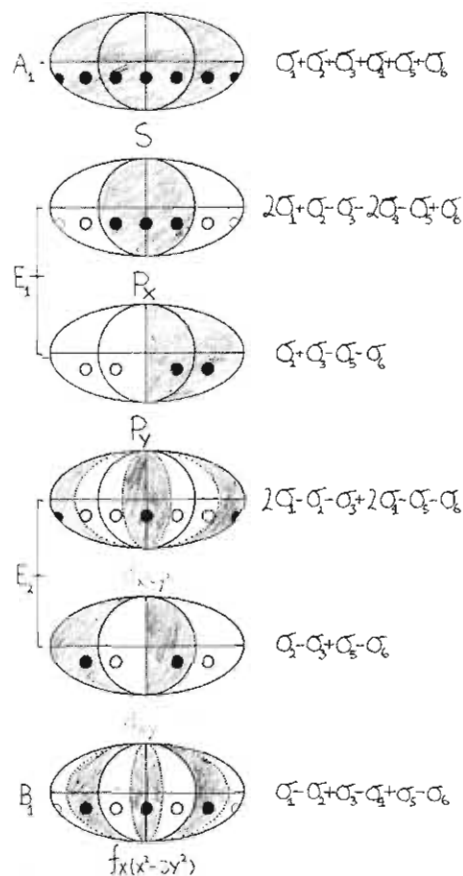


Figure 7.  $\sigma$ -group orbitals in  $C_{6v}$  symmetry as Mollweide projections.

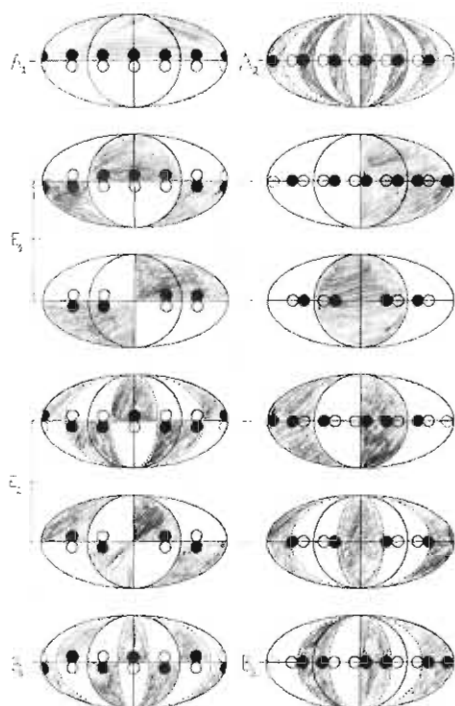


Figure 8.  $\pi$ -orbitals in  $D_{6h}$  symmetry as Mollweide projections. This set also can be used for  $C_{3v}$  structures, thereby preserving the conventional separation of  $\pi^g$  and  $\pi^u$  components. Note again the alignments of the local components with respect to the great circles of symmetry or antisymmetry.

the determination of the local resultant gradient directions at the ligand positions, and so it is difficult to recognize and distinguish repetitions of symmetries merely due to the mappings from  $R_3$  onto the lower order group in question. Our

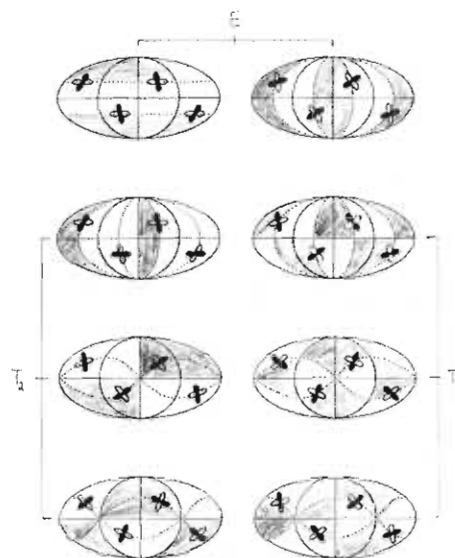


Figure 9. Hypothetical  $\delta$ -type interactions of a  $T_d$ -symmetry ligand field. The irreducible symmetries E,  $T_2$ , and  $T_1$  are the same as is found for  $\pi$ -type interactions. The E set of group orbitals interconvert on local  $45^\circ$  rotations while the  $T_2$  set first encountered for the  $d_{xy}$ , and  $d_{yz}$  central functions yield the  $T_1$  set of  $f_{x(x^2-y^2)}$ ,  $f_{x(y^2-z^2)}$ , and  $f_{y(z^2-x^2)}$  central function symmetry, and the great circles of symmetry of the  $T_2$  type central functions become great circles of antisymmetry.

procedure is equivalent to the analysis directly on the basic set of Mollweide projections of the special  $C_{nv}$  geometries that are of the higher symmetries  $D_{nh}$  since this is inherent in the ligand geometry alone. This point is emphasized in Figure 8 by the presentation of the group orbitals superimposed on the equatorial great circles of the appropriate same-symmetry central harmonic projections, which procedure maintains the rule that individual components lie along axes of symmetry and lie normal to axes of antisymmetry.

#### $\delta$ -Orbitals and Metal-Metal Bonds

The general procedures that we have established for the generation of  $\sigma$ - and  $\pi$ -type orbitals also apply for the generation of  $\delta$ -type group orbitals in which local ligand d atomic orbitals are disposed to be coincident with lines of longitude and latitude ( $\delta_l^{\theta^2-\phi^2}$ ) or at  $\pi/4$  ( $\delta_l^{\theta\phi}$ ) to such lines on the unit sphere through ligand positions. The central function property that determines the resultant  $\delta$ -component direction at each ligand position for a given symmetry is its concavity, which is determined by second derivatives with respect to  $\theta$  and  $\phi$ . Stone<sup>7</sup> has given tensor harmonics of this fashion which yield the directions of greatest concavity as linear combinations of the basic  $\delta_l^{\theta^2-\phi^2}$  and  $\delta_l^{\theta\phi}$  functions at each ligand position. Implicit in these results too is our rule concerning the orientation of the resultant functions when the ligand positions lie on great circles which are axes of symmetry or antisymmetry.<sup>8</sup> For  $\delta$ -type interactions resultant d functions lie in the directions of greatest concavity when aligned along lines of symmetry through ligand positions or at  $\pi/4$  to lines of antisymmetry through ligand positions. Each kind of resultant combination generated in this fashion yields complementary functions on local rotation of the individual components through  $\pi/4$ .

These statements are illustrated for the hypothetical case of  $\delta$ -type interactions for a  $T_d$ -symmetry ligand field in Figure 9. Since the tensor harmonics depend on the second derivatives of the central generating functions, the  $\delta$  analysis is started from the d central functions. Note the interconversion as in the  $\pi$  case of the two e-type symmetry functions and the exclusion of the  $f_{xyz}$  ( $A_1$ ) symmetry since the ligand positions correspond to maxima of the central function amplitudes, so that there is a net zero contribution of the  $\delta$  component at each ligand site.

Table III. Components of the Various Molecular Orbitals for the  $[\text{Re}_2\text{Cl}_8]^{2-}$  Ion Matched according to the Generating Central Harmonic Function<sup>a</sup>

generator	$\text{Re}_2$	$\text{Cl}_8$	type of interaction
s	$6s/5d_{z^2}/6p$	$3p\sigma$	$\sigma$
$p_x/p_y$	$6p_x/6p_y$	$3p\sigma$	$\sigma(\text{Re-Cl})$
$p_z$	$5d_{xz}/5d_{yz}$	$3p\sigma$	$\pi(\text{Re-Re})$
	$6s/5d_{z^2}/6p\sigma$	$3p\sigma$	$\sigma^*(\text{Re-Re})$
$d_{x^2-y^2}$	$5d_{x^2-y^2}$	$3p\sigma$	$\sigma(\text{Re-Cl})$
		$3p\sigma$	$\delta(\text{Re-Re})$
$d_{xy}$	$5d_{xy}$	$(3p\pi)$	$\delta(\text{Re-Re})$
$d_{xz}/d_{yz}$	$6p_x/6p_y$	$3p\sigma$	$\sigma(\text{Re-Cl})$
	$5d_{xz}/5d_{yz}$	$3p\sigma$	$\pi^*(\text{Re-Re})$
$f_{(x^2-y^2)z}$	$5d_{x^2-y^2}$	$3p\sigma$	$\sigma(\text{Re-Cl})$
		$(3p\pi)$	$\delta^*(\text{Re-Re})$
$f_{xyz}$	$5d_{xy}$	$(3p\pi)$	$\delta^*(\text{Re-Re})$

<sup>a</sup> It is assumed that the chlorine  $p\sigma$  orbitals are substantially more important than the chlorine  $p\pi$  in the determination of the structure stability.

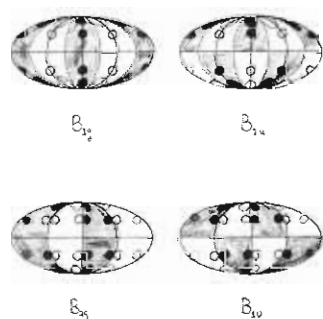


Figure 10.  $\delta$ -type d-orbital interactions in the  $[\text{Re}_2\text{Cl}_8]^{2-}$  ion. The quadruple bond between the rhenium  $d_{xy}$  interactions stabilizes the eclipsed  $D_{4h}$  geometry of the ion.

Two important classes of molecular material in which metal-metal bonds with  $\delta$ -type d-orbital interactions are to be expected are the binuclear metallic species exemplified by the octachlorodirhenate(2-) ion,  $[\text{Re}_2\text{Cl}_8]^{2-}$ ,<sup>9,10</sup> and the transition-metal atom clusters that are components of, for example, the complex ion  $[\text{Mo}_6\text{Cl}_8]^{4+}$ <sup>11</sup> or primitive models for the surface regions of bulk metals.<sup>12-15</sup> The classification and discussion of the molecule or cluster wave functions for such systems is facilitated by our projection technique.

The eclipsed ( $D_{4h}$ ) structure of the  $[\text{Re}_2\text{Cl}_8]^{2-}$  ion is attributed to the stability of the Re-Re  $\delta$  bond, consistent with the short metal bond observed. For eight  $p\sigma$  orbitals on the chlorine atoms, bonding interactions are possible with the rhenium valence s, p, and d orbitals of suitable energies and symmetries which also are required to provide the metal-metal bonding. The symmetry requirements follow directly from a Mollweide projection analysis for the ion structure components of two rhenium atoms surrounded by eight chlorine atoms arranged in  $D_{4h}$  symmetry. The classification of the group orbital components is given in Table III, and the important  $\delta$ -type interactions are shown in Figure 10. The eclipsed structure of the ion is stabilized by both the  $\delta$ -type rhenium  $5d_{xy}$  interactions between the chlorine atom positions with presumably some chlorine  $p\pi$  contributions and the mixing of rhenium  $5d_{x^2-y^2}$  with the chlorine  $p\sigma$  orbitals.

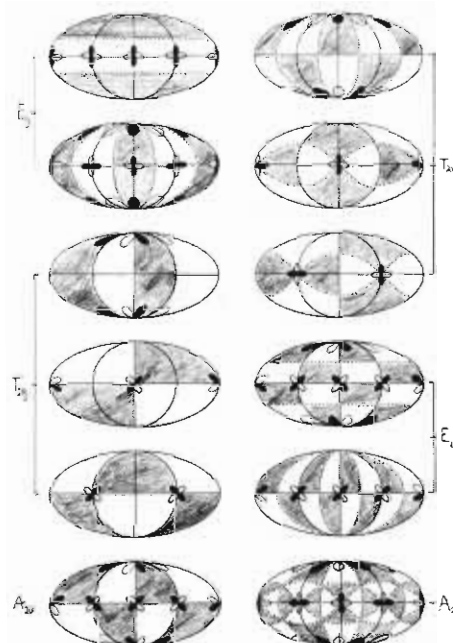


Figure 11.  $\delta$ -type interactions of an  $M_6$  cage in such complex ions as  $[\text{Mo}_6\text{Cl}_8]^{4+}$  and  $[\text{Nb}_6\text{Cl}_{12}]^{2+}$ . Note that for  $d\delta$  orbitals the net overlap at local atomic positions with the phases of the central function on a projection is often different from that found for  $p\pi$  orbitals. Thus in the second diagram of this figure the equatorial  $d\delta$  set do contribute to the  $e_g$  group orbital. For the conventional orientations of the  $d\delta$  orbitals, the 12 group orbitals given are identical with those given in ref 17.

In Figure 11 the  $\delta$ -type group orbitals for an  $M_6$  octahedral metallic cluster are classified. Two features are particularly evident from an inspection of the projections. It is straightforward to count the number of bonding and antibonding interactions in any of the molecular orbitals if such criteria are to be used to assess the orbital energies and so determine the cluster electronic configuration. It is clear that bonding interactions to an  $M_6$  cage from surrounding ligands should lead to facial attachments (8 ligands) when the  $d_{xy}$  orbitals of the cage are involved and to edge attachment (12 ligands) when the cage to ligand bonding is dominated by the  $d_{x^2-y^2}$  orbitals of the cage. Just such a distinction is found, for example, in the clusters  $[\text{Mo}_6\text{Cl}_8]^{4+}$ <sup>11</sup> and  $[\text{Nb}_6\text{Cl}_{12}]^{2+}$ ,<sup>16</sup> for which the cage electron configurations are  $(a_{1g}\sigma)^2(t_{1u}\pi)^6(t_{2g}\pi)^6(e_g\delta)^2(t_{2u}\delta)^6$  and  $(a_{1g}\delta)^2(t_{1u}\pi)^6(t_{2g}\pi)^6(a_{2u}\delta)^2$ , respectively.<sup>17</sup>

Note that in both these cases involving  $D_{4h}$  and  $D_h$  symmetries the rotation rule for the generation of new  $\delta$ -orbital symmetries can be used. Thus in Figure 10 the  $d_{x^2-y^2}$  functions on the rhenium atoms generate the  $d_{xy}$ -based functions in the lower diagrams by rotation locally through  $45^\circ$ . In Figure 11 the  $\delta$ -type cluster orbitals obtained in sequence from the basic Mollweide projection sets also exhibit the same rotational relationships. Note also the manner in which the relationships between the central, surface, and tensor harmonics determine the level at which group orbitals match the symmetries of the central harmonic functions. For  $\sigma$  interactions the values of the central function at the ligand positions determine the coefficients of  $\sigma$  components; thus the s central harmonic is relevant to these cases. For  $\pi$  components the gradient relationship excludes the s central harmonic, while for  $\delta$  interactions the second-derivative relationship means that only projections of  $l \geq 2$  level central harmonics can contribute.

- (9) F. A. Cotton, *Inorg. Chem.*, **4**, 334 (1965).  
 (10) F. A. Cotton and C. B. Harris, *Inorg. Chem.*, **6**, 924 (1967).  
 (11) F. W. Koknat and R. E. McCarley, *Inorg. Chem.*, **13**, 295 (1974).  
 (12) R. P. Messmer, *Surf. Sci.*, **106**, 225 (1981).  
 (13) R. P. Messmer, C. W. Tucker, Jr., and K. H. Johnson, *Surf. Sci.*, **42**, 341 (1974).  
 (14) C. M. Quinn and N. V. Richardson, *Faraday Discuss. Chem. Soc.*, No. **60**, 201 (1975).  
 (15) C. M. Quinn and M. E. Schwartz, *J. Chem. Phys.*, **74**, 5181 (1981).

- (16) B. G. Hughes, J. L. Meyer, P. B. Fleming, and R. E. McCarley, *Inorg. Chem.*, **9**, 1343 (1970).  
 (17) K. F. Purcell and B. Kotz, "Inorganic Chemistry", W. B. Saunders, Philadelphia, 1977.